Structural Insights into the Exchange Domain of Sec2p: Expression, Purification, Crystallization, and Preliminary X-Ray Diffraction Data Analysis

Harindarpal S. Gill*

Department of Cellular and Molecular Physiology, Yale University School of Medicine, 333 Cedar Street, New Haven, CT 06520, USA

Abstract: Sec2p is an essential yeast gene and is part of the cell polarization process that leads to budding. The N-terminal domain of sec2p (Sec2pN)—the guanine-nucleotide exchange factor for sec4p—has been expressed in *Escherichia coli*, purified, and crystallized. Crystals belong to the space group $P2_1$ with unit cell dimensions 178.1 x 98.4 x 180.0 Å, $\beta = 91.7^{o}$, and diffract synchrotron-generated X-rays to better than 3.6 Å resolution. Pseudo-precession plots reveal a Laue symmetry of 2/*m*, corresponding to the aforementioned space group, and unusual weak diffraction in the ~5–7 Å resolution range. The Matthews number calculations for a typical crystal density suggest a range of 28 to 64 molecules per asymmetric unit. Self-rotation and native Patterson calculations demonstrate a pure helical array of protein subunits. Based on the X-ray diffraction data analysis and amino-acid sequence alignments, the paper presents a hypothetical model of the exchange domain of sec2p as a pair of coiled-coil helices that binds to sec4p and facilitates nucleotide disassociation.

Keywords: Pseudo-precession plot, Laue symmetry, self-rotation function, non-crystallographic symmetry, coiled-coil, nucleotide exchange factor.

INTRODUCTION

Sec2p plays a role in transporting secretory vesicles from the Golgi to the cell surface of *Saccharomyces cerevisiae* during cell growth. The N terminus of sec2p, NtSec2p residues 1−160, has been identified as an exchange factor for sec4p, which is also required for polarized transport of post-Golgi vesicles [1,2,3,4,5]. Functionally, NtSec2p preferentially binds sec4p in a nucleotide-free conformation state and facilitates GDP dissociation from sec4p when in the nucleotide-bound state [2,3,4]. From the crystal structures of sec4p [6], an interaction between phenylalanine residues 40 and 173 coordinates the binding and release of GDP, which is associated with conformational changes in loop residues 48 to 56 termed "Switch I" [7]. Structurally, based on sequence analysis, NtSec2p is predicted to be a coiled-coil [2,8], with each coil characterized to be amphipathic by helical-wheel plots [9]. Recently, the structures of other exchange factors have been elucidated, such as sec5 [10] and rabex-5 [11,12], although their overall tertiary-folds are different than that expected for NtSec2p. Elucidation of the NtSec2p structure would thus be the first representative member in its family [2]. The paper here reports on: (1) an expression and purification system that yields large soluble amounts of the NtSec2p; (2) the crystallization conditions that lead to X-ray diffracting crystals of the NtSec2p; (3) the properties of the crystals; (4) and the first evidence for a strict helical-based tertiary-fold for NtSec2p.

*Address correspondence to this author at the Department of Cellular and Molecular Physiology, Yale University School of Medicine, 333 Cedar Street, New Haven, CT 06520, USA; Tel: 203-785-2356; Fax: 203-785-4951; E-mail: hs.gill@yale.edu

METHODS AND MATERIALS

Construction of the sec2p Expression Vector

The full-length sec2p gene isolated from *Saccharomyces cerevisiae* was donated by Peter Novick, 333 Cedar Street, Yale School of Medicine, New Haven, Connecticut, USA 06510. Two forward primers were synthesized to construct a Sec2pN plasmid that either encoded for residues 17-160 or 24-160 of sec2p. Each contained a NcoI restriction site immediately merged into either a glycine or a valine codon followed by a six-histidine codon stretch that proceeded the 17^{th} or 24^{th} codon of sec2p, respectively: 5'-CATGCCATGGGACATCATCATCATCATTCTACGCAATTGATCGAG-3' and 5'-CATGCCATGGTGCATCATCATCATCATAGCGTGGATAAACAGTCACACACTTAG-3'. The reverse primer contained a stop-codon after the 160^{th} codon of sec2p and an XhoI restriction site thereafter: 5'-GTCCTCGAGTTAACTATGCATCACTTTTTTCAG-3'. Reaction mixtures for the polymerase chain reaction were made according to the manufacture's protocol for Cloned-Pfu™ and contained 1× supplied buffer, 100 ng template, 1 μm each primer, 0.2 mM each dNTP, in a 50 μl final volume. Programming of the thermal cycler (PTC, Biorad, CA) consisted of 1 cycle for 72 ^{o}C for 10 min., 4^{o}C thereafter. DNA products were then subcloned into the NcoI and XhoI restriction sites of the pET15B (Novagen, Madison, WI) bacterial expression vector, thereby making a short, non-cleavable histidine-tagged fusion of the corresponding N-terminal version of sec2p, which will be both referred to here as Sec2pN.

Expression and Purification of Sec2pN

Sec2pN was expressed in *Escherichia coli* strain Rosetta™ (Novagen, Madison, WI), which contains an addi-

0929-8665/07 $50.00+.00

tional plasmid that encodes for six eukaryotic tRNAs. Cells were grown at 37 ^{o}C in a shaker until an OD_{600} of 1, at which point the temperature was lowered to 15 ^{o}C. Cells were induced with 0.5mM IPTG, harvested after 12 hours, and visually checked for over-expression of ~16 kDa product on SDS-PAGE. The cells were resuspended in a volume of two times the wet-cell gram weight with buffer containing 20 mM Tris pH 8, 300 mM NaCl, and 4.4 mM $MgCl_2$. Lysozyme was added to a final concentration of 1 mg/ml and incubated for 1 hour at 4 ^{o}C. The cells were further disrupted by sonication and spun down at 10,000 ×g. The supernatant was then applied over a Ni^{2+}-resin with a bed-volume of 1 ml per 10-12 mg protein. The resin was washed with buffer containing 20mM imidazole pH 8, and the protein was eluted with buffer containing 300 mM imidazole pH 8. Elution samples were combined and concentrated using a concentration unit with a 30 kDa MW cut-off. After overloading a SDS-gel with 8 to 40 μg Sec2pN and performing SDS-PAGE, Coomassie-staining revealed no other bands. Sec2pN concentrations were judged by comparison with BSA standards on SDS-PAGE, because of low absorbance by UV-spectrophotometric methods and poor color development by Bradford reagent (Biorad, CA). The sample was also applied to an analytical Superdex-200 HR 10/30 gel-filtration column (Amersham Pharmacia), in part to judge the molecular mass of the Sec2pN. The molecular-mass protein standards and their respective retention volumes used in estimating molecular mass were thyroglobulin, 600 kDa, 8.5 ml; bovine γ-globulin, 158 kDa, 11.5 ml; chicken ovalbumin, 44 kDa, 14.3 ml; and equine myoglobin, 15 kDa, 16.5 ml.

Crystallization of Sec2pN

Crystal conditions were screened using the Hampton I & II (Hampton Research, Irvine, CA) and Wizard I & II (de-Code Genetics, Bainbridge Island, WA) screening kits. Crystals were grown by the hanging-drop and vapor-diffusion method [13]. The buffer of the protein solution contained 20 mM Tris pH 8.0, 300 mM NaCl, and 2.2 mM $MgCl_2$. Each drop had a total volume of 4 μl, consisting of equal parts of well-solution and a 50-75 mg/ml Sec2pN stock solution. The volume of the well was 0.5 ml.

X-Ray Data Collection and Processing

Cryogenic data were initially recorded in-house on a R-axis II detector with a rotating anode X-ray generator (Rigaku Corporation, Shibuya, Tokyo). The well-solution was suitable as a cryoprotectant. Synchrotron-generated data were subsequently obtained using a Quantum 3 x 3 detector (Area Detector System Corporation) at the National Synchrotron Light Source (NSLS) at the X25 beamline, Brookhaven, Long Island, NY USA. The oscillation angle was 1^{o} and each frame was exposed for 40 sec. The crystal-to-detector distance was 450 mm. A 90^{o} sweep yielded complete data within 45 min. Data were processed with HKL2000 [14].

RESULTS AND DISCUSSION

Expression and Purification of Sec2pN

The approach detailed in *Methods & Materials*—slow growth of *E. coli* with induction at 15 ^{o}C—led to soluble protein for both versions of Sec2pN (i.e., residues 17-160 and 24-160). The yield was ~100 mg protein per 10 g *E. coli* cell paste. Purification—using Ni^{2+}-column affinity chromatography followed by gel-filtration chromatography—resulted in a purity of >99% of Sec2pN. Fig. **1** demonstrates that the Ni^{2+}-resin is singly responsible for the high purity. The retention volume (12.8 ml) from the size exclusion corresponds to a molecular mass of ~85 kDa. This molecular mass would roughly correspond to a pentamer, although the elongated-shape of Sec2pN predicted from sequence analysis [2] complicates the determination of oligomer state from size-exclusion chromatography. Moreover, Sec2pN could be concentrated to high concentrations (75 mg/ml), which were needed to grow the diffracting quality crystals described below.

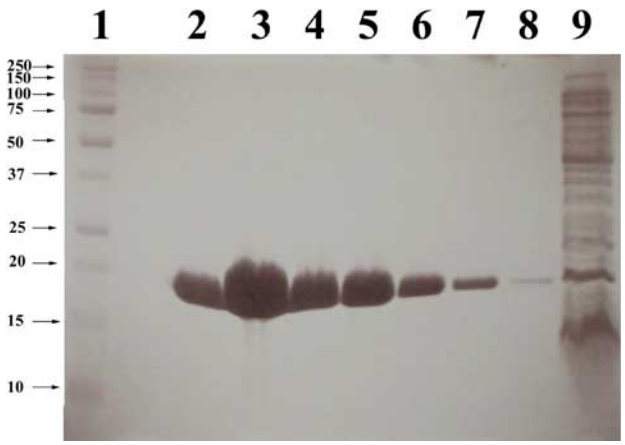

Figure 1. SDS-PAGE of Pure Sec2pN protein. Elution fractions of Sec2pN after the Ni^{2+}-affinity chromatography step are shown. Lane 1, molecular-weight markers; Lane 2-8, one to 80 μg of Sec2pN, with the elution peak in lane 2; Lane 9, supernatant after whole-cell lysis.

Crystal Forms of Sec2pN

Sec2pN crystallized in several different morphological forms, two of which are shown in Fig. **2**. Either truncation

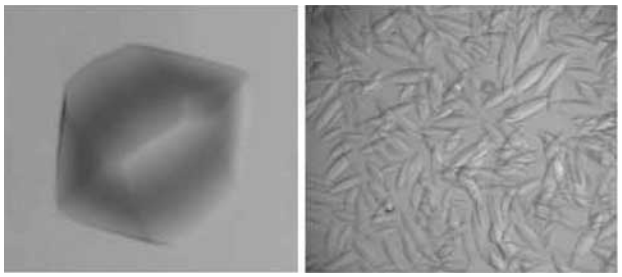

Figure 2. Crystals of Sec2pN. Two extreme examples of Sec2pN crystals are shown. Left: A Sec2pN crystal grown in the presence of MPD polarizes light. The crystal belongs to space group $P2_1$ and is the form used in data collection here. Dimensions typically vary from 0.1 mm to 0.5 mm in each direction. Right: Sec2pN crystals grown in the presence of a number of volatile alcohols appear boat-shaped. These crystals can be stained with methyl-violet dye and grow within a day. They yield ringed, powder-like type of X-ray diffraction (not shown), suggesting an extreme random-order of molecules in the crystal lattice.

length described in *Methods & Materials* yielded similar crystals. The solution that yielded the best crystals quality consisted of 17% (v/v) 2-methyl-2,4-pentanediol, 0.2 M trisodium-citrate dehydrate pH 5.5, and 0.1 M ammonium acetate. Concentrations of Sec2pN below 10 mg/ml in drops gave small crystals immediately that yielded poor to no X-ray diffraction. High concentrations gave large bipyramid-shaped crystals that diffracted X-rays to better than 3.6 Å resolution, after three months of growth at room temperature.

X-Ray Data Collection

The crystals diffract X-rays to 3.6 Å resolution. The cell parameters are given in Table **1**. Crystals belong to space group $P2_1$, which is part of the monoclinic crystal system. Fig. **3** shows pseudo-procession plots that reveal Laue symmetry of 2/*m*, demonstrating the packing arrangement of a crystal formed by the monoclinic crystal system. The number of molecules per asymmetric unit, which range from 28 to 64 by Matthew's calculation (V_M) [15,16], is in the range of V_M values of 1.6 $Å^3$/Da for densely packed crystals to 3.6 $Å^3$/Da for moderately loosely packed crystals. The number of molecules in the asymmetric unit may actually be lower than those values suggested by the V_M. As shown in Fig. **4**, Sec2pN may be similar to a large group of structural and cytoskeletal proteins, such as tropomyosin, whose quaternary structures are organized as a coiled-coil arrangement of helical-pairs. Their crystal packings can have V_M values > 4. For Sec2pN, a V_M of ≥ 4 would correspond to ≤ 20 molecules per asymmetric unit for example.

Table 1. Sec2p Crystal Parameters*

Source	X25
Radiation Wavelength	1.1 Å
Resolution Range	50.0–3.6 Å
Space Group	$P2_1$
Unit Cell Dimensions	a = 178.1 Å
	b = 98.4 Å
	c = 180.0 Å
	β = 91.7°
Mosaicity	0.370
Completeness (%)	99.0 (97.4)
Observed Reflections	268,562
Unique Reflections	72,052
Redundancy	3.7 (3.5)
R_{sym} (%)‡	6.6 (27.6)
Overall I/σ	25.5 (4.7)

* Values in parentheses refer to the highest-resolution shell

‡ Rsym = ∑hkl∑I|Ii(hkl) - <I(hkl)>|/ ∑hkl∑II(hkl)I, where Ii(hkl) is the ith measurement and <I(hkl)> is the mean of all measurements of I(h) for Miller indices h, k, l.

Self-Rotation Function

To determine the presence of non-crystallographic symmetry elements, arising from the contents or molecules within the asymmetric unit, self-rotation functions [17] were calculated. In the κ = 180 section (Fig. **5**), we find an arc of seven dyads along a great circle, although the limited clarity here may mask additional peaks. The dyads are perpendicular to the expected crystallographic twofold symmetry at (0,0) arising from the space group $P2_1$, which likely masks another dyad. And in the κ = 30 to 180 sections, we find additional peaks at (0,0). The patterns of peaks described above are consistent with a cylindrical or helical arrangement of a molecule whose long axis points along the **b**-axis. Further, Native Patterson maps demonstrate seven molecules of translational symmetry at fractional coordinates (0.13 0.5 0.5), (0.5 0.5 0.85), (0 0.46 0.0), (0.38 0.0 0.345), (0.38 0.0 0.625), (0.12 0.04 0.50), (0.50 0.04 0.85) whose peaks are above a 5σ threshold. Because there are indeed multiple copies in the asymmetric unit, the self-rotation function tells that all helical molecules extend in the same direction, arrayed in discrete positions.

What Does the Self-Rotation of Other Helical Proteins Look Like?

To demonstrate that the contents of the asymmetric unit of the Sec2pN crystals do indeed conform to a helical structure, (Fig. **5**) compares the observed self-rotation peaks with calculated self-rotation peaks of a single chained, helical-bundle[1] structure and of two classic coiled-coil[2] structures. As expected, both the calculated self-rotation of the helical-bundle and the coiled-coils show an arc of dyads, which are perpendicular to another dyad as well as to peaks in the κ = 30 to 180 sections. Moreover, when the helical-bundle is arrayed in a crystal lattice of the monoclinic crystal system, as taken from the crystallization report from Kavori *et al* [18], the self-rotation contains a similar low resolution-looking arc to the self-rotation of Sec2pN. That is, the self-rotation contains seven apparent but evenly spaced dyads that at the time suggested a sevenfold screw rotation axis of the molecule. The crystal also has a similarly broad range of V_M values to the one described here. It appears that the helical-bundle is arrayed in the crystal varying in rotations along its long axis that gave it its apparent sevenfold-symmetry, since the structure was eventually elucidated to be a four-helical bundle. Likewise for Sec2pN, because of the broad range of possible molecules in the asymmetric unit and the lack of clarity of the self-rotation, the exact oligomerization or helical symmetry of Sec2pN will require solving the structure.

How Does NtSec2p Compare with Other Known Exchange Factors?

Sequence comparisons suggest that NtSec2p is unusual among other eukaryotic exchange factors whose crystal structures have been solved, such as sec5 [10] and rabex-5 [11,12]. NtSec2p at best shares an identity of 27.3% with rabin-8, an exchange factor for rab-8 in humans and whose structure has also yet to be determined. The moderate sequence identity, which falls into an ambiguous range of accepted values of 20-30% that we term "twilight-zone,"

[1] The helical-bundle is taken from the C-terminus of the Rous Sarcoma Virus capsid protein [18], which was solved by NMR methods. (See PDBid: 1EOQ)

[2] Modeled from tropomyosin (PDBid:1C1G)

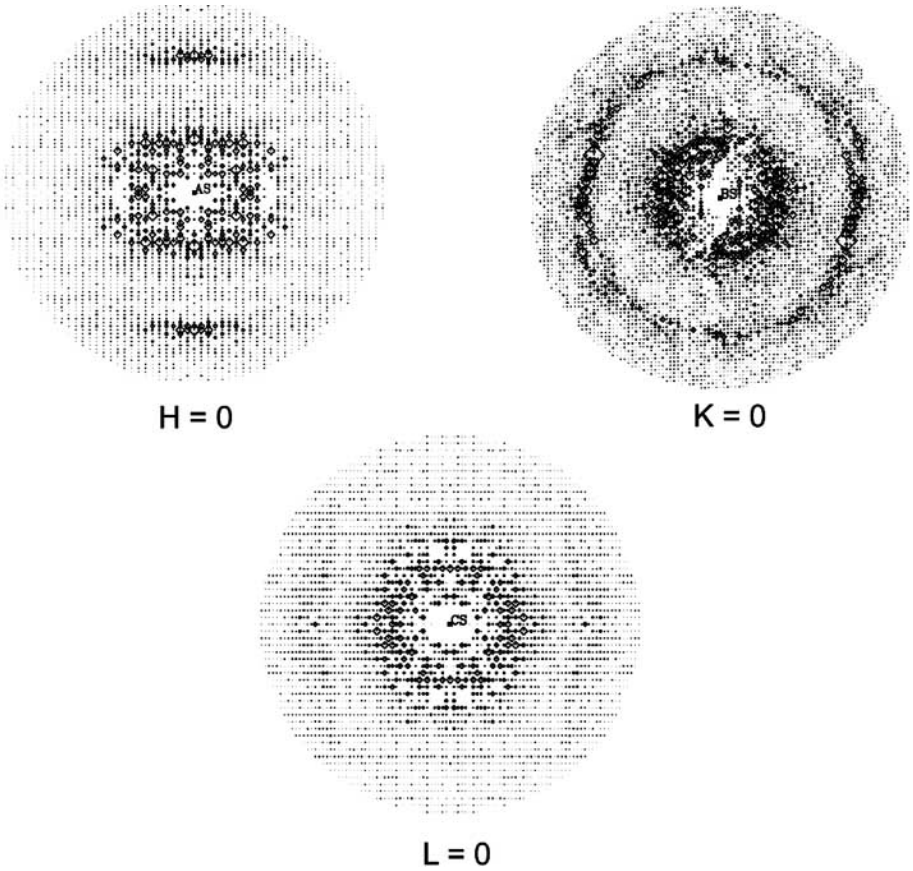

Figure 3. H = 0, K = 0, L = 0 sections of the reciprocal lattice. The sections were simulated with the program HKLPLOT [21] from full three-dimensional data. X-ray diffraction data to 3.6 Å resolution were collected from single Sec2pN crystal at 100K. **(H = 0)** In the 0KL section of the reciprocal lattice, the **c***-axis is vertical and the **b***-axis is horizontal. **(K = 0)** In the H0L section, the **a***-axis is vertical and the **c***-axis is horizontal. **(L = 0)** In the HK0 section, the **a***-axis is vertical and the **b***-axis is horizontal. Boxes are drawn to aid in the observation of symmetry elements within the sections. Note that both the 0KL and HK0 sections contain mirrored-symmetry about the **a***- and **c***- axes. On the other hand, in the H0L section we can only see twofold symmetry parallel to the **b***-axis (BS), thereby ultimately demonstrating a monoclinic crystal system. In addition, the observed systematic absences of the form (2n+1) along the **b***-axis correspond to a screw-axis in the crystal lattice, defining the $P2_1$ space group. Interestingly, the plots also show a drop in intensity between the resolution range ~5–7 Å, which may reflect the stacked helical content in the asymmetric unit.

```
       10         20         30         40         50         60         70         80
NtSec2 SVDKQSHLEEQLNKSLKTIASQKAAIENYNQLKEDYNTLKRELSDRDDEVKRLREDIAKENELRTKAEEEADKLNKEV
       :  : ..:::.:.   ... : .:  :.:.: .. :.   . :::.  :..  : ..:...   :: :.  : :. :.
Tropo  SEGKCAELEEELKTVTNNLKSLEAQAEKYSQKEDKYEEEIKVLSDKLKEAET-RAEFAERS--VTKLEKSIDDLEDEL
          40         50         60         70         80         90         100        110

      60         70         80         90
NtSec2 REDIAKENELRTKAEEE-ADKLNKEVEDLTAS
       ::.  :  . . . . : :..:..: :.  ::
Rabex5 REEYHKARQKQIQEDWELAERLQREEEEAFAS
       40         50         60         70
```

Figure 4. Amino-acid sequence alignments to known helical proteins. **(TOP)** Of known structure, NtSec2p is most similar to rabbit skeletal α-tropomyosin (PDBid:2D3E), which is a coiled-coil pair of helices. NtSec2p shares a 30.8% identity with tropomyosin over a 78 amino-acid overlap. A coiled-coil pair of helices like tropomyosin would be consistent with sequence analysis results that predict that NtSec2p is a coiled-coil dimer rather than a trimeric one. **(BOTTOM)** Despite its overall low amino-acid sequence identity with bovine rabex-5, NtSec2p does share a short segment of sequence identity to a domain of rabex-5, which is strictly a helical rod as opposed to a coiled-coil. In particular, the sequence corresponding to residues 60 to 90 of sec2p has a 31.2% identity to the ubiquitin-binding motif (D-x-x-LA-x-x-L-x-x-E-E) of rabex-5 that is also characterized to be an amphipathic helix.

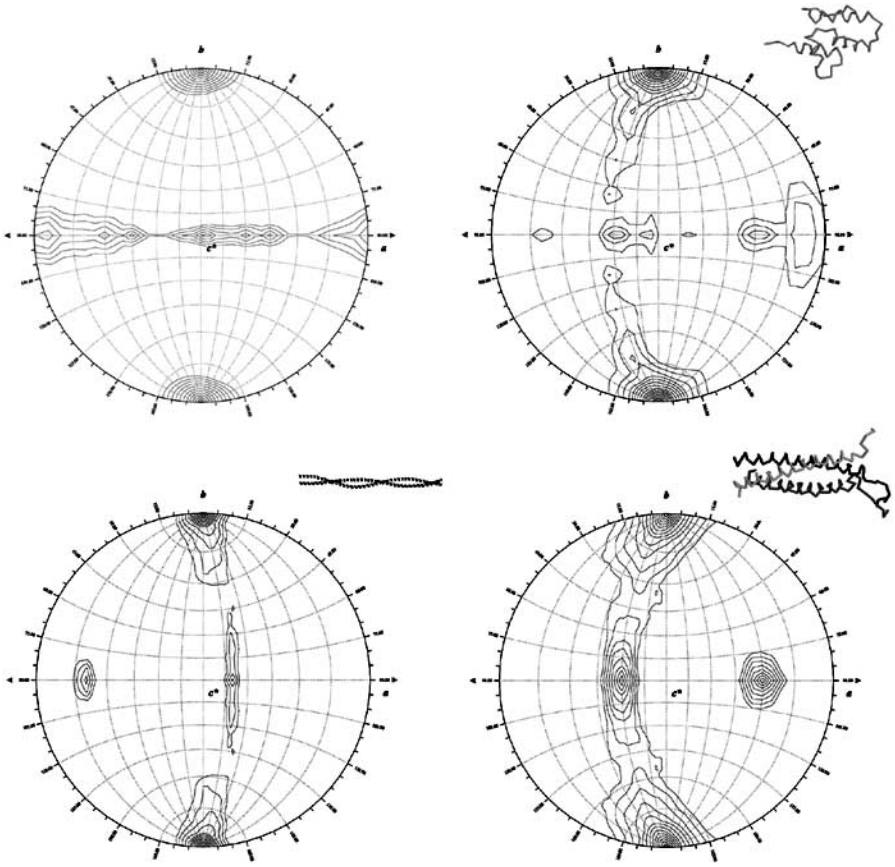

Figure 5. Observed self-rotation of Sec2pN vs. calculated self-rotation examples of a four-helical bundle and coiled-coiled helices. In the κ = 180 sections shown, the ψ-axis is along the circumference and φ-axis is along the equator. A resolution range of 4–20 Å and radii of 12–48 were explored. In (A), the Sec2pN self-rotation is shown. Seven apparent quasi-dyads are seen in the figure, which was generated with a radii of 40, lying along $\psi = 90^{o}$ with some spaced every 15^{o} apart in φ, at (ψ,φ) = (0,90), (45,90), (60,90), (85,90), (135,90), (150, 90), (175,90). A crystallographic peak, arising from the rotational symmetry of the monoclinic crystal system, at (0,0) or (180,0) is orthogonal to each dyad and likely masks another dyad arising from the helical molecules. In (B), (C), and (D), the calculated self-rotation functions for a four-helical bundle, a coiled-coil dimer, and a coiled-coil trimer are respectively shown. The molecules used to generate the self-rotation function are shown above each figure and were placed in a monoclinic cell with their long axes pointing approximately along the a-axis to unmask the additional dyad. Note the similarity of peaks among the calculated self-rotation functions with the observed self-rotation function of Sec2pN. Also, note that the actual model used to calculate the self-rotation function for the coiled-coil trimer was a NMR family of overlapping models, giving rise to broad peaks like those generated by the multiple molecules in the asymmetric unit of the Sec2pN crystals. The self-rotation functions were calculated with the program GLRF [22].

makes it difficult to judge a structural similarity. Still, both N-terminal domains of sec2p and rabin-8 have a similar predicted [19,20] pattern of helical regions (not shown), which suggests a close relationship of their three-dimensional folds. In addition, both are predicted to be coiled-coils [2]– in agreement with their high percent (>30%) shared identity in amino-acid sequence alignments with tropomyosin shown in Fig. **4**.

How Could a Helical Structure Facilitate GDP Disassociation from sec4p?

Because sequence analysis predicts that the tertiary fold of NtSec2p is likely to be a coiled-coil [2], consistent with the X-ray diffraction data presented here, we can begin to examine possible interactions with its binding partner sec4p. A hypothetical dimerized coiled-coil model of NtSec2p, for example, could compete for the binding pocket of the C-terminal helix of sec4p (residues 168 to 186), disrupting key protein-protein interactions as seen in sec4p-nucleotide complexes [7]. Here we can envision that the native, unbound state of sec4p to have a loose C-terminal helix. Because of the ease of accessibility, a coiled-coil (NtSec2p) may bind the empty surface cavity formed from a β-sheet of sec4p, preventing the C-terminal helix from closing into its pocket. Alternatively when the helix is sitting in its cavity and GDP is bound as seen in the crystal structures on which these models are partially based [6], NtSec2p could simply bind the helix and loosen it from the pocket. This disruption in interaction between F40 and F173 on the helix would trigger a conformational change in loop residues 48 to 56 (referred to as Switch I) and prevent key interactions between the loop and the nucleotide base, releasing GDP. In another example, a helical structure might directly compete for the nucleotide-binding site, which would also be in theoretical agreement

for NtSec2p preference for binding the sec4p in the nucleotide-free state.

DISCLOSURES

The crystallization work was supported by a PEW fellowship to Dr. Karin M. Reinisch. X-ray data for this study were measured free-of-charge at the NSLS that is supported by the Offices of Biological and Environmental Research and Basic Energy Sciences of the US-DOE, and the from the National Center for Research Resources of NIH.

REFERENCES

[1] Novick, P., Field, C. and Schekman, R. **(1980)** *Cell, 21*, 205-215.
[2] Ortiz, D., Medkova, M., Walch-Solimena, C. and Novick, P. **(2002)** *J. Cell Biol., 157*, 1005-1015.
[3] Bielli, P., Casavola, E. C., Biroccio, A., Urbani, A. and Ragnini-Wilson, A. **(2006)** *Mol. Microbiol., 59*, 1576-1590.
[4] Walch-Solimena, C., Collins, R. N. and Novick, P. J. **(1997)** *J. Cell Biol., 137*, 1495-1509.
[5] Medkova, M., France, Y. E., Coleman, J. and Novick, P. **(2006)** *Mol. Biol. Cell, 17*, 2757-2769.
[6] Stroupe, C. and Brunger, A. T. **(2000)** *J. Mol. Biol., 304*, 585-598.
[7] Neuwald, A. F., Kannan, N., Poleksic, A., Hata, N. and Liu, J. S. **(2003)** *Genome Res., 13*, 673-692.
[8] Nair, J., Muller, H., Peterson, M. and Novick, P. **(1990)** *J. Cell Biol., 110*, 1897-1909.
[9] Brondyk, W. H., McKiernan, C. J., Fortner, K. A., Stabila, P., Holz, R. W. and Macara, I. G. **(1995)** *Mol. Cell Biol., 15*, 1137-1143.
[10] Fukai, S., Matern, H. T., Jagath, J. R., Scheller, R. H. and Brunger, A. T. **(2003)** *EMBO J., 22*, 3267-3278.
[11] Lee, S., Tsai, Y. C., Mattera, R., Smith, W. J., Kostelansky, M. S., Weissman, A. M., Bonifacino, J. S. and Hurley, J. H. **(2006)** *Nat. Struct. Mol. Biol., 13*, 264-271.
[12] Penengo, L., Mapelli, M., Murachelli, A. G., Confalonieri, S., Magri, L., Musacchio, A., Di Fiore, P. P., Polo, S. and Schneider, T. R. **(2006)** *Cell, 124*, 1183-1195.
[13] McPherson, A., Malkin, A. J. and Kuznetsov, Y. G. **(1995)** *Structure, 3*, 759-768.
[14] Otwinowski, Z., Borek, D., Majewski, W. and Minor, W. **(2003)** *Acta Crystallogr. A, 59*, 228-234.
[15] Kantardjieff, K. A. and Rupp, B. **(2003)** *Protein Sci., 12*, 1865-1871.
[16] Matthews, B. W. **(1968)** *J. Mol. Biol., 33*, 491-497.
[17] Rossmann M and Blow D **(1962)** *Acta Crystallographica, 15*, 24-31.
[18] Kovari, L. C., Momany, C. A., Miyagi, F., Lee, S., Campbell, S., Vuong, B., Vogt, V. M. and Rossmann, M. G. **(1997)** *Virology, 238*, 79-84.
[19] Rost, B. and Sander, C. **(1993)** *J. Mol. Biol., 232*, 584-599.
[20] Przybylski, D. and Rost, B. **(2002)** *Proteins, 46*, 197-205.
[21] Collaborative Computational Project, N. 4. **(1994)** *Acta Cryst. D, 50*, 760-763.
[22] Tong, L. and Rossmann, M. G. **(1997)** *Methods Enzymol., 276*, 594-611.

Received: June 05, 2006 **Revised: December 31, 2006** **Accepted: January 10, 2007**